Interaction of Fibrin(ogen) with the Endothelial Cell Receptor VE-Cadherin: Mapping of the Receptor-Binding Site in the NH_2-Terminal Portions of the Fibrin β Chains†

Sergei Gorlatov and Leonid Medved*

Department of Biochemistry, the Holland Laboratory, American Red Cross, Rockville, Maryland 20855

Received December 11, 2001; Revised Manuscript Received January 23, 2002

ABSTRACT: Interaction of fibrin with endothelial cells stimulates capillary tube formation thus promoting angiogenesis. This interaction occurs via endothelial cell receptor VE-cadherin and fibrin β chain 15−42 regions [Bach, T. L., et al. (1998) *J. Biol. Chem. 272*, 30719−30728]. To clarify the mechanism of this interaction, we expressed in *Escherichia coli* a number of recombinant fibrin(ogen) fragments containing the β15−42 region or the VE-cad(1−2) and VE-cad(1−4) fragments encompassing two and four extracellular NH_2-terminal domains of VE-cadherin, respectively, and tested interaction between them by surface plasmon resonance and ELISA. Neither the recombinant Bβ1−57 or Bβ1−64 fragments, nor β15−57 or β15−64 prepared from the latter fragments by thrombin treatment to remove fibrinopeptides B, bound the recombinant VE-cadherin fragments. At the same time, a dimeric recombinant thrombin-treated $(\beta15-66)_2$ fragment, which had been disulfide-linked via Cys65 to mimic the dimeric arrangement of the β chains in fibrin, bound VE-cad(1−4) well, but not VE-cad(1−2); no binding was observed with the untreated $(B\beta1-66)_2$ dimer. We next mutated several residues in the dimer, His16, Arg17, Pro18, and Asp20, and tested the interaction of the thrombin-treated mutants with VE-cad(1−4) by ligand blotting and surface plasmon resonance. No binding was observed with the H16A and R17Q single mutants and the H16P, P18V double mutant while the P18A and D20N single mutants bound VE-cad(1−4) with the same affinity as the thrombin-treated wild-type dimer. These results indicate that the VE-cadherin binding site in fibrin includes NH_2-terminal regions of both fibrin β-chains, that His16 and Arg17 are critical for the binding, and that the third and/or fourth extracellular domains of VE-cadherin are required for the binding to occur.

Fibrinogen is a plasma protein that after thrombin-mediated removal of its fibrinopeptides A and B spontaneously forms a fibrin gel that prevents the loss of blood upon vascular injury. Besides its prominent role in hemostasis, fibrin(ogen) has been also recognized as an adhesive protein that interacts with various cell types. Fibrin gel serves as a provisional matrix on which various cell types adhere, migrate, and proliferate during different physiological and pathological processes. Among them is angiogenesis, or formation of new blood vessels, that plays an important role in wound healing, tissue repair, tumorigenesis, and some cardiovascular diseases (*1*−*4*).

Angiogenesis is stimulated by numerous factors that promote interaction of endothelial cells with each other and with extracellular matrix molecules, resulting in formation of capillary tubes. It was shown that fibrin gels induce an angiogenic response that was enhanced when certain chemoattractants or mitogens were included in the gels (*5*). It was also demonstrated that under serum-free conditions the endothelial cell monolayer sandwiched between two fibrin gels rearranges rapidly into an extensive network of capillary-like tubes (*6*), reinforcing the previous finding (*5*) that fibrin itself can induce angiogenesis. The mechanism of this induction remains unclear.

Fibrinogen is a chemical dimer consisting of three pairs of polypeptide chains, Aα, Bβ, and γ, whose NH_2-terminal portions are disulfide-linked in the central portion of the molecule (*7*). Fibrin-stimulated angiogenesis was found to be dependent on the thrombin-mediated exposure of the NH_2-terminal 15−42 portion of its β chains since neither des-A fibrin, in which fibrinopeptides B (residues Bβ1−14) were not removed, nor fibrin-325, which lacks these portions, stimulated capillary tube formation (*6*). A Sepharose-coupled peptide mimicking β15−42 sequence of fibrin was shown to bind a 130-kDa receptor on endothelial cells (*8*). An endothelial cell receptor of similar size that interacted specifically with the fibrin(ogen)-derived BrCN-fragment N-DSK[1] containing this sequence was identified later as VE-cadherin (*9*). VE-cadherin (or vascular endothelial cadherin) is a transmembrane protein expressed by vascular endothelial cells. It is a member of the cadherin family of cell−cell

† This work was supported by National Institutes of Health Grant HL-56051 (to L.M.)

* To whom correspondence should be addressed: The Holland Laboratory, American Red Cross, 15601 Crabbs Branch Way, Rockville, MD 20855. Phone: (301) 738−0719. Fax: (301) 738−0740. E-mail: medvedL@usa.redcross.org.

[1] N-DSK, NH_2-terminal disulfide knot of fibrinogen; PVDF, poly(vinylidene difluoride); SPR, surface plasmon resonance; TBS, tris buffer saline (20 mM Tris buffer, pH 7.5, 150 mM NaCl); PMSF, phenylmethanesulfonyl fluoride; DTT, dithiothreitol.

10.1021/bi0160314 CCC: $22.00
Published on Web 03/03/2002

adhesion receptors with a typical modular structure that includes cytoplasmic, transmembrane, and five homologous extracellular domains (*10*). VE-cadherin mediates cell−cell contacts at intercellular junctions via homophilic interactions between its extracellular domains (*11*) and plays a critical role in the maintenance and restoration of endothelium integrity (*12*). This receptor seems to mediate fibrin- and collagen-induced endothelial cell capillary tube formation since this process was inhibited by a monoclonal antibody directed against its extracellular domains (*13*). Thus, interaction of VE-cadherin with fibrin through the β15−42 sequence of the latter may contribute to the mechanism through which fibrin induces angiogenesis (*9*, *13*). A better understanding of this interaction is required to elucidate this mechanism.

There are at least two more endothelial cell receptors besides VE-cadherin, namely, integrin $\alpha_V\beta_3$ and nonintegrin intercellular adhesion molecule-1 (ICAM-1), that were implicated in interaction with different regions of fibrin(ogen) (*14*−*17*). In addition, fibrin may interact with endothelial cell surface proteoglycans through its heparin-binding domain (*18*). These complicate direct measurements of VE-cadherin-mediated interaction between endothelial cells and fibrin. To overcome this problem, we expressed in a bacterial system variants of the NH_2-terminal portion of fibrin(ogen) β chain containing β15−42 sequence as well as variants of VE-cadherin including its two and four extracellular domains and studied the interactions between them. The results indicate that the fully active VE-cadherin-binding domain of fibrin must contain NH_2-terminal portions of both β chains and that the third and/or fourth extracellular domains of VE-cadherin are required to preserve fibrin-binding activity of VE-cadherin. We also identified by site-directed mutagenesis those amino acid residues in the β15−42 region of fibrin that are critical for binding to VE-cadherin.

EXPERIMENTAL PROCEDURES

Proteins and Peptides. Plasminogen-depleted human fibrinogen was purchased from Enzyme Research Laboratories. Human plasmin, bovine α-thrombin, and chicken egg albumin were from Sigma. Natural Bβ1−42 peptide corresponding to the NH_2-terminal region of fibrinogen Bβ chain was prepared from a plasmin digest of fibrinogen as described in ref *19*. Synthetic peptide β15−42 corresponding to the NH_2-terminal region of fibrin β chain was synthesized by SynPep (Dublin, CA).

Antibodies. Mab-1, a Ca^{2+}-dependent mouse monoclonal antibody against extracellular domains of human VE-cadherin (catalog no. RDI-VECADHabm) was from Research Diagnostics Inc (Flanders, NJ). Mab-2, mouse monoclonal antibody against fibrin neotope on β chain (product 350), was from American Diagnostica Inc. (Greenwich, CT).

Expression of Recombinant Fibrin(ogen) Bβ15−42 Containing Fragments. Recombinant fragments including human fibrinogen Bβ chain regions 1−57, 1−64, and 1−66, with a single Cys residue at position 65, were produced in *Escherichia coli* using pCAL-n expression vector. The cDNA fragments encoding these regions were produced by polymerase chain reaction (PCR) using as a template full-length cDNA encoding the human fibrinogen Bβ-chain, which was kindly provided by Dr. S. Lord (*20*). The following oligonucleotides were used as primers: 5′-GATGACGACCATATGCAAGGTGTCAACGACAATGAG-3′ (forward primer for all fragments), 5′-CATCAGAAGCTTATCTTTCTACTTTCTTTTGAGTG-3′(reverse primer for Bβ1−57), 5′-GGAACAAAAGCTTAGCCTCCAGCATCAGGGGCTTTTC-3′ reverse primer for Bβ1−64), and 5′-CGGAAAGCTTAGCCACAGCCTCCAGCATCAGGGGCTTTTC-3′ (reverse primer for Bβ1−66). The forward primer incorporated the *Nde*I restriction site immediately before the coding region; the final three bases of the *Nde*I site, ATG, coded for the fMet initiation residue. The reverse primers included a TAA stop codon and *Hind*III restriction site. The coding sequence for BβLeu66 was replaced by that coding Gly to mimic COOH-terminus of glutathion (γGlu−Cys−Gly) to enhance the formation of disulfide bond. The amplified cDNA fragments were digested with *Nde*I and *Hind*III restriction enzymes and ligated into pCAL-n expression vector. The resulting plasmids were used for transformation DH5a and then BL21(DE3) *E. coli* host cells. All cDNA fragments were sequenced in both directions to confirm the integrity of the entire coding sequences. For expression of the Bβ chain fragments, the plasmid containing BL21(DE3) cells were grown for 2 h at 37 °C in Luria broth medium containing 50 mg/L ampicillin, induced with 0.4 mM isopropyl-1-thio-β-D-galactopyranoside for 4−5 h, harvested by centrifugation, and frozen.

Purification and Thrombin Cleavage of the Recombinant Fibrin(ogen) Fragments. The recombinant Bβ1−57 and Bβ1−64 fragments were purified in a similar manner. Frozen cells were thawed, suspended in purification buffer (50 mM Tris, pH 7.5, 1 mM EDTA, and 0.1 mM PMSF) containing 1 mM DTT, sonicated, and centrifuged. The supernatant was fractionated with ammonium sulfate, and the fraction precipitated between 40 and 60% saturation was further fractionated on Phenyl-Sepharose. The nonbound material, which contained mainly the recombinant Bβ1−57 or Bβ1−64 fragment, was then applied on DEAE-Sepharose column equilibrated with purification buffer. The purified fragment was recovered in the nonbound fraction, which was concentrated and further purified on Superdex-75. The $(B\beta1-66)_2$ dimer was purified by a similar procedure except that 1 mM DTT was present at each stage including the DEAE-Sepharose chromatography to prevent disulfide formation via Cys65. The monomeric Bβ1−66 fragment was then dialyzed extensively against 20 mM Tris buffer, pH 8.0, containing 150 mM NaCl and 0.02% NaN_3, to form a disulfide-bridged dimer, $(B\beta1-66)_2$, followed by further purification on Superdex-75. All purified fragments were concentrated on Centricon-10 and stored frozen at −80 °C. The final yield of the purified fragments was 15−20 mg/L of bacterial culture.

To produce thrombin cleaved species, β15−57, β15−64, and $(\beta15-66)_2$, the recombinant fragments at 10 mg/mL were dialyzed into 10 mM HEPES buffer, pH 7.4, containing 150 mM NaCl and 0.02% NaN_3, and treated with thrombin at 5 NIH U/mL for 1 h at 37 °C followed by gel filtration on Superdex-75.

Site-Directed Mutagenesis. All mutants of the $(B\beta1-66)_2$ dimer were produced by site-directed mutagenesis. The single mutants, H16A and P18A, and the double mutant, H16P, P18V, were produced by using Transformer site-directed mutagenesis kit (Clontech). The pCAL-n construct containing

DNA encoding the Bβ1−66 region was modified by using following mutagenic primers:

5′-CAATGAGGAAGGTTTCTTCAGTGCCCGCG-GTgcTCGACCCCTTG-3′ (H16A);

5′-CAATGAGGAAGGTTTCTTCAGTGCCCGCG-GTCATCGAgCCCTTGACAAG-3′ (P18A);

5′-CAATGAGGAAGGTTTCTTCAGTGCCCGCG-GTCcTCGAgtCCTTGACAAG-3′ (H16P, P18V);

The R17Q and the D20N mutants were produced by using Quick-Change kit (Stratagene). The pCAL-n construct was modified by using following mutagenic primers:

5′-GGTTTCTTCAGTGCCCGCGGTCATCaAC-CCCTTGACAAG-3′ and

5′-CTTGTCAAGGGGTtGATGACCGCGGGCACTGA-AGAAACC-3′ (forward and reverse primers, respectively, for the R17Q mutant); 5′-GGTTTCTTCAGTGCCCGC-GGTCATCGACCCCTTaACAAGAAGAGAG-3′ and 5′-CTCTCTTCTTGTtAAGGGGTCGATGACCGCGGGCA-CTGAAGAAACC-3′ (forward and reverse primers, respectively, for the D20N mutant). These primers introduced the desired mutations (the lowercase letters indicate the mutagenic bases) and the unique *Sca*II restriction site (underlined) to facilitate further analysis. Some primers also eliminated the unique *BseR*I restriction site (double underlined) for primary selection purpose. After elongation of DNA by T4 DNA polymerase (Clontech) or PfuTurbo DNA polymerase (Stratagene), the mixture of template and mutated plasmids was treated with *BseR*I or *Dpn*I, respectively, to selectively digest the template, and transformed into a *mutS E. coli* strain defective in mismatch repair. The desired plasmids were further selected by restriction analysis with *Sca* II and transformed into DH5α *E. coli* cells. After each mutation was confirmed by sequencing the entire DNA fragment, the BL21(DE3) *E. coli* host cells were transformed with the mutant plasmid and the $(B\beta1-66)_2$ mutants were expressed, purified, and activated with thrombin by the procedures described above for the wild-type dimer.

Expression and Purification of Recombinant VE-Cadherin Variants. Recombinant VE-cadherin fragments, VE-cad(1−2) and VE-cad(1−4), including amino acid residues 1−209 and 1−434, respectively, were produced in *E. coli* using pET-20b expression vector. The cDNA fragments encoding these regions were produced by PCR using as a template the full-length cDNA encoding human VE-cadherin that was kindly provided by Dr. J. Martinez (*21*). The following oligonucleotides were used as primers:

5′-GATCGCCAACATATGGATTGGATTTGGAACCA-GATG-3′, the forward primer for both fragments, which incorporated the *Nde*I restriction site immediately before the coding region; the final three bases of the NdeI site, ATG, coded for the fMet initiation residue. The reverse primer for the fragment encoding VE-cad(1−4), 5′-GCTGCTCGAGCT-TGGCAAACTCCGGGGCATTG-3′, contained *Xho*I restriction site resulting in the recombinant product with a His-tag at the COOH-terminus. The reverse primer for the fragment encoding VE-cad(1−2), 5′-CGGACTCGAGTTAGGGGAA-GTTGTCATTGATGTC-3′, contained in-frame stop codon followed by *Xho*I restriction site; the presence of the former prevented translation of the plasmid's His-tag coding sequence. The amplified cDNA fragments were digested with *Nde*I and *Xho*I restriction enzymes and ligated into pET-20b expression vector. The resulting plasmids were used for transformation of DH5α and then BL21(DE3) *E. coli* host cells. Both cDNA fragments were sequenced in both directions to confirm the integrity of the entire coding sequences. For expression of the protein fragments, the plasmids containing BL21(DE3) cells were grown for 2 h at 37 °C in Luria broth medium containing 50 mg/L ampicillin, induced with 0.4 mM isopropyl-1-thio-β-D-galactopyranoside for 4−5 h, harvested by centrifugation, and frozen.

The recombinant VE-cad(1−2) and VE-cad(1−4) fragments were purified in a similar manner. Frozen cells were thawed, suspended in 20 mM Tris buffer, pH 7.5, containing 1 mM DTT, 0.1 mM PMSF, and protease inhibitor cocktail (Roche), followed by sonication and centrifugation. The pellet, containing mainly the fragments of interest, was washed four times with 20 mM Tris buffer, pH 7.5, containing 1 mM EDTA, 0.5 M urea, and 0.5% Triton X-100. The pellet was then dissolved in 20 mM Tris buffer, pH 7.5, 150 mM NaCl (TBS) containing 8 M urea, and the fragments were purified on Superdex 200 column equilibrated with 20 mM Tris buffer, pH 7.5, containing 5 M urea, 0.5 M NaCl, and 1 mM EDTA. The fragments were dialyzed into TBS containing 1 mM $CaCl_2$ and 0.02% NaN_3 and further purified by gel filtration on a Superdex 200 column equilibrated with 10 mM Hepes buffer, pH 7.4, containing 200 mM NaCl, 1 mM $CaCl_2$, and 0.02% NaN_3. Both fragments were concentrated and stored frozen at −80 °C. The final yield of the purified fragments was 15−20 mg/L of bacterial culture.

Protein Concentration Determination. Concentrations of the recombinant fragments and the natural and synthetic peptides were determined spectrophotometrically using extinction coefficients ($E_{280,1\%}$) calculated from the amino acid composition by the following equation: $E_{280,1\%} = (5690W + 1280Y + 120S\text{-}S)/(0.1M)$, where W, Y, and S-S represent the number of Trp and Tyr residues and disulfide bonds, respectively, and M represents molecular mass (*22*, *23*). Molecular masses of the fragments and peptides were calculated based on their amino acid composition.

Fluorescence Study. Fluorescence spectra were recorded in an SLM 8000-C fluorometer. Fluorescence measurements of thermal-induced unfolding were performed by monitoring the ratio of fluorescence intensity at 370 nm to that at 330 nm with excitation at 280 nm in the same fluorometer. Temperature was controlled with a circulating water bath programmed to raise the temperature at about 1 °C/min. Protein concentrations were 0.02−0.03 mg/mL.

Solid-Phase Binding Assay. The interaction between the recombinant fibrin(ogen) fragments and the VE-cad(1−4) fragment was studied by ELISA using plastic microtiter plates (Fisher). Wells of microtiter plates were coated overnight at 4 °C with the recombinant fibrin(ogen) fragments in 100 mM $NaHCO_3$ buffer, pH 9.4, at 10 μg/mL. The wells were then blocked with SEA BLOCK Blocking Reagent (Pierce) at 37 °C for 2 h. Following washing with 20 mM Tris buffer, pH 7.5, containing 150 mM NaCl and 0.05% Tween-20, the indicated concentrations of the recombinant VE-cad(1−4) fragment in binding buffer (10 mM HEPES, pH 7.4, with 200 mM NaCl, 1 mM $CaCl_2$, 0.02% NaN_3, and 0.05% β-octyl-glucoside) was added to the wells and incubated overnight at 4 °C. After washing with binding buffer, bound VE-cad(1−4) was measured by the reaction of its His-tag with a nickel-activated derivative of horseradish peroxidase (INDIA HisProbe-HRP, Pierce) in 20 mM

potassium phosphate buffer, pH 7.4, containing 450 mM NaCl and 0.05% Tween-20. A TMB Microwell Peroxide substrate (Kirkegaard & Perry Laboratories Inc.) was added to the wells, and the amount of bound HisProbe-HRP was measured spectrophotometricaly at 450 nm. Data were analyzed by nonlinear regression analysis using eq 1:

$$B = B_{max}/(1 + K_d/[L]) \quad (1)$$

were B represents the amount of ligand bound, B_{max} is the amount of ligand bound at saturation, [L] is the molar concentration of free ligand, and K_d is dissociation constant.

BIAcore Analysis. The interaction between the recombinant fragments was also studied by surface plasmon resonance (SPR) using the BIAcore 3000 biosensor (BIAcore AB, Uppsala, Sweden), which measures association/dissociation of proteins in real time (*24*, *25*). The fragments, VE-cad-(1−2) and VE-cad(1−4), and ovalbumin were covalently coupled via ϵ-amino groups to the activated surface of a CM5 biosensor chip by the procedure described in ref *24*. Briefly, the carboxyl groups on the sensor surface were activated with an injection of a solution containing 0.2 M *N*-ethyl-*N*-(3-diethylamino-propyl) carbodiimide and 0.05 M *N*-hydroxy-succinimide. The proteins to be coupled were prepared in 10 mM sodium-acetate buffer, pH 4.0, containing 1 mM $CaCl_2$, and injected onto the activated CM5 surface at 5 μL/min followed by incubation for 7 min after which the surface was deactivated by passing 1 M ethanolamine. Activation time, ligand concentration, and contact time were adjusted to achieve a coupling density of 5−6 ng/mm^2. Binding experiments were performed in 10 mM Hepes buffer, pH 7.4, containing 200 mM NaCl, 1 mM $CaCl_2$, 0.02% NaN_3, and 0.05% *n*-octyl β-D-glucopyranoside (binding buffer). Samples at different concentrations were injected in duplicate in at least three separate experiments and the association−dissociation between the immobilized and the added proteins was monitored as the change in the SPR response. To regenerate the chip, complete dissociation of the complex was achieved by adding 20 mM Tris buffer, pH 7.5, containing 0.5 M urea, 0.5 M NaCl, and 0.5% Triton X-100, for 1 min following reequilibration with binding buffer. Experimental data were analyzed using BIAevaluation 3.0 software supplied with the instrument. Briefly, kinetic constants, k_{ass} and k_{dis}, were estimated by global analysis of the association/dissociation curves to the 1:1 Langmurian interaction model (*26*). The dissociation equilibrium constant (K_d) was calculated as $K_d = k_{diss}/k_{ass}$.

IAsys Analysis. Some SPR experiments were performed using the IAsys biosensor (Fisons, Cambridge, UK) (*25*). Fibrinogen or the recombinant $(\beta 15-66)_2$ fragment was covalently coupled via ϵ-amino groups to the activated CM-Dextran sensor surface of the IAsys biosensor cuvette at a coupling density of 9−15 ng/mm^2 exactly as described in ref *27* except that sodium-acetate buffer used for the coupling was at pH 5.0 instead of pH 4.5. To convert immobilized fibrinogen into fibrin, the former was treated with thrombin at 0.1 NIH U/mL for 30 min. Binding experiments were performed in the same binding buffer as above. Samples at different concentrations were injected in duplicate in two separate experiments and the association−dissociation between the immobilized and the added proteins was monitored as the change in the SPR response. To regenerate the chip, complete dissociation of the complex was achieved by adding 3 M guanidinium chloride for 0.5 min following reequilibration with the binding buffer. The traces of the association processes were recorded and the data were analyzed using the FASTfit kinetics analysis software supplied with the instrument as previously described in detail (*27*). Briefly, the association curves at each concentration of ligand were fitted to the pseudo-first-order equation to derive the observed rate constant, k_{obs} (termed on-rate constant in FASTfit). Then the concentration dependence of k_{obs} was fitted to eq 2:

$$k_{obs} = k_{diss} + k_{ass}[\text{ligand}] \quad (2)$$

to find the association rate constant (k_{ass}) from the slope and the dissociation rate constant (k_{diss}) from the intercept. The dissociation equilibrium constant was calculated as $K_d = k_{diss}/k_{ass}$.

Ligand Blotting Assay. Detection of VE-cad(1−4) bound to the wild type and the mutant $(\beta 15-66)_2$ fragments was performed using NuPAGE BisTris electrophoretic system according to the Western transfer protocol (Invitrogen). The wild type and the mutant $(\beta 15-66)_2$ fragments were subjected to electrophoresis, and electrotransferred to a poly-(vinylidene difluoride) (PVDF) membrane (Invitrogen). To check the effectiveness of the protein transfer, the membrane was stained with 0.5% Ponceau S for 1 min followed washing with deionized water and destaining with TBS. The membrane then was blocked overnight with Sea Block (Pierce) followed by washing with TBS containing 0.05% Tween 20. Binding was performed in binding buffer containing 400 nM VE-cad(1−4) at room temperature for 5 h. Bound VE-cad(1−4) was detected via its His-tag by reaction with INDIA HisProbe-HRP (Pierce) and visualized by using SuperSignal West Pico Chemiluminescent Substrate (Pierce) as recommended by the manufacturer.

RESULTS

To map the VE-cadherin-binding site in the central region of fibrin(ogen), it was important to select an appropriate model that would allow manipulation of the sequence forming this region and direct testing of its interaction with VE-cadherin. Since the 15−42 region of fibrin(ogen) Bβ chains has been implicated in binding with VE-cadherin (*6*), we prepared a number of fragments containing this region.

Preparation and Characterization of the β15−42-Containing Fibrin(ogen) Fragments. The alignment of all three fibrinogen chains shows that the interchain sequence homology, which is often used to delineate structural/functional domains, starts at residues AαLys29, BβLys58, and γTyr1, and that Aα1−28 and Bβ1−57 are extra residues that are missing in the homologous γ chain (Figure 1A). The crystal structure of the central region of fibrinogen also revealed that these extra residues of the Bβ chain do not contribute to the compact central funnel domain (*28*, *29*). This suggests that the Bβ1−57 portion may represent a more complete structural/functional unit denoted here as BβN-domain, which after activation could be functionally superior to the β15−42 peptide used in the previous studies. In agreement, it is well established that the Bβ1−53 regions are usually removed upon digestion of fibrinogen with plasmin (*7*). It was also predicted based on theoretical analysis of the primary structure that the Bβ1−55 portion could be folded

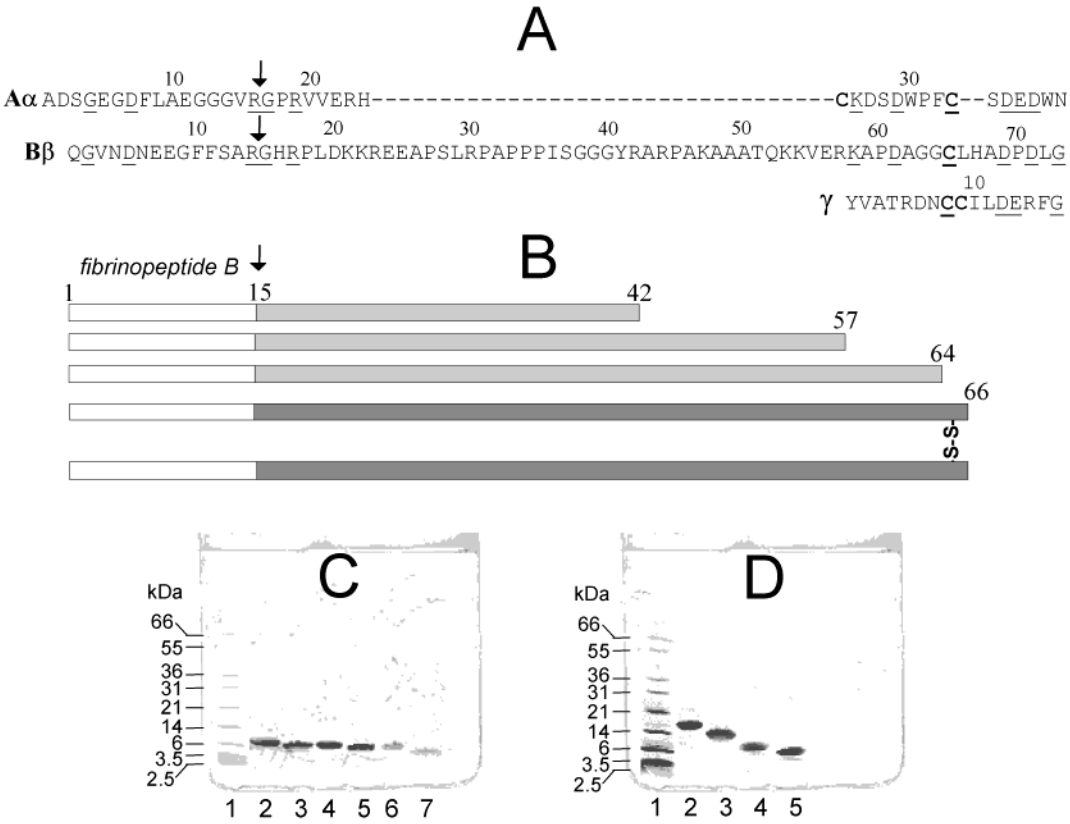

FIGURE 1: Schematic representation of the β15−42 containing fibrin(ogen) fragments and their SDS−PAGE analysis. Panel A, alignment of the NH_2-terminal portions of human fibrinogen Aα, Bβ, and γ chains. Arrows indicate thrombin cleavage sites. Panel B, a diagram of the β15−42 containing fragments prepared in this study. Open boxes represent fibrinopeptide B cleaved by thrombin, while filled boxes represent thrombin-activated fragments. S-S represents disulfide bond connecting two polypeptides via Cys65. Panel C shows SDS electrophoresis in gradient 8−25% polyacrylamide gel of the recombinant fragments Bβ1−64, β15−64, Bβ1−57, and β15−57 (lanes 2, 3, 4 and 5, respectively), and proteolytic fragment Bβ1−42 (lane 6) and synthetic peptide β15−42 (lane 7). Panel D shows SDS electrophoresis in 8−25% polyacrylamide gel of the recombinant dimeric $(B\beta1-66)_2$ fragment, nonreduced and reduced (lanes 2 and 4, respectively); lanes 3 and 5 represent, respectively, the nonreduced and reduced thrombin-activated $(\beta15-66)_2$ dimer. Lane 1 in panels C and D contain molecular mass protein markers (Mark 12 Unstained Standard, Novex).

into a compact structure (*30*). These facts were used for selection of the boundaries for the BβN-domain variants to be expressed.

Three recombinant fragments, Bβ1−57 corresponding exactly to the "extra" portion of the Bβ chain, Bβ1−64, which ends just before the first naturally occurring BβCys65, and Bβ1−66 that includes this Cys (Figure 1B−D) were expressed in *E. coli* (see Experimental Procedures). The latter was purified in reducing conditions to prevent disulfide bond formation and then oxidized to form a disulfide-linked dimer, $(B\beta1-66)_2$. This dimer mimics the central region of fibrin(ogen) that contains two NH_2-terminal portions of the Bβ chains, each disulfide-linked to the Aα chain via BβCys65−AαCys36 (*28*, *29*). All fragments were treated with thrombin to remove fibrinopeptides B and to produce the monomeric β15−57 and β15−64 fragments, and the dimeric $(\beta15-66)_2$ fragment. It should be noted that our attempts to express for comparison a shorter version of this region, Bβ1−42, failed. Although the resulting pCAL-n expression vector contained the insert encoding this fragment, as revealed by sequence analysis, no protein product corresponding to this peptide was detected in bacterial lysate. Instead, we purified this fragment from a plasmin digest of fibrinogen and also prepared the synthetic β15−42 peptide (see Experimental Procedures).

To check the folding status of the recombinant Bβ fragments, we used differential scanning calorimetry and circular dichroism (CD). No denaturation transition was detected in the temperature range 10−120 °C when the Bβ1−57, Bβ1−64, or $(B\beta1-66)_2$ fragments were heated in the calorimeter (not shown), suggesting that neither monomers nor dimers form a compact structure. In agreement, their CD spectra (not shown) were typical for an unfolded protein indicating the absence of a secondary structure. Nevertheless, further experiments revealed that the VE-cadherin binding properties were preserved in at least one of the fragments (see below).

Preparation and Characterization of the Recombinant Variants of VE-Cadherin. Although purification of VE-cadherin from endothelial cell culture or placenta using affinity chromatography on β15−42 peptide-Sepharose or anti-VE-cadherin Mab-Sepharose was reported earlier (*8*, *11*), the yield was very low. Our attempt to purify VE-cadherin from placenta using a combination of these methods also produced very low yields; the amount of the resulting protein was sufficient only to immobilize it on a BIAcore sensor chip and to identify it with anti-pan-cadherin antibody (not shown). To overcome this problem, we expressed in *E. coli* two variants of the extracellular portion of VE-cadherin, including residues 1−209 and 1−434. The latter, denoted here as VE-cad(1−4) includes four of the five extracellular domains of the receptor, while the former, denoted as VE-cad(1−2), contained two such domains (Figure 2A). Both recombinant fragments were found mainly in inclusion bodies

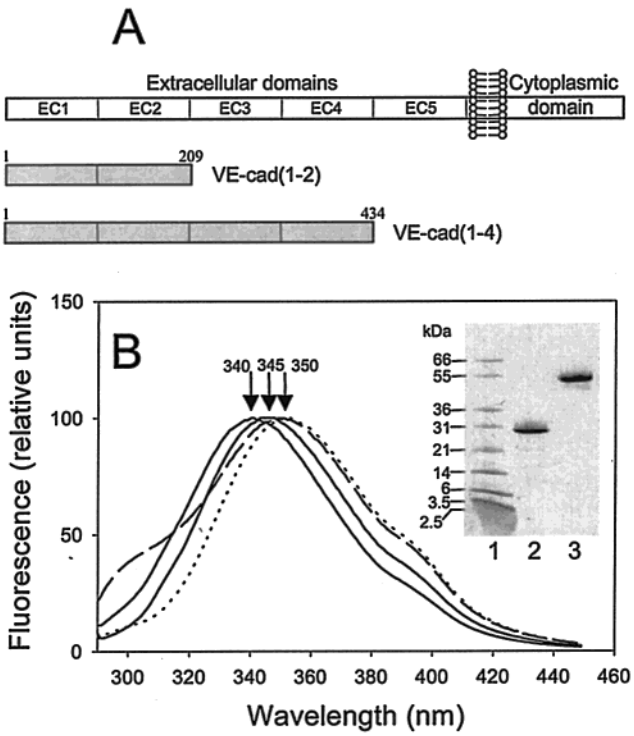

FIGURE 2: Schematic representation of VE-cadherin and its recombinant fragments, and their SDS−PAGE and fluorescence analysis. Panel A, a diagram of VE-cadherin consisting of five homologous extracellular domains (EC1 through EC5), transmembrane domain and COOH-terminal cytoplasmic domain, and the recombinant fragments VE-cad(1−2) and VE-cad(1−4) consisting of two and for extracellular domains, respectively. Panel B, the normalized fluorescence spectra of VE-cad(1−2) and VE-cad(1−4) in 8 M urea before refolding (broken and dotted lines, respectively) and after refolding in 20 mM HEPES buffer, pH 7.4, containing 200 mM NaCl and 1 mM $CaCl_2$ (solid lines with maxima at 345 and 340 nm, respectively). Inset shows SDS-electrophoresis in 8−25% polyacrylamide gel of the VE-cad(1−2) and VE-cad(1−4) fragments (lanes *2* and 3, respectively); lane 1 contains molecular mass protein markers (Mark 12 Unstained Standard, Novex).

from which they were purified to homogeneity and refolded (Figure 2B, inset) as described in Experimental Procedures.

Since VE-cad(1−2) and VE-cad(1−4) were expressed in a bacterial system and denaturing concentrations of urea were used upon their purification, it was important to characterize their structural integrity, i.e., the presence of compact structure. To check their folding status, we used fluorescence spectroscopy since, in contrast to the recombinant variants of the BβN-domain, they both contain several Trp residues. In 8 M urea, both VE-cad(1−2) and VE-cad(1−4) fragments exhibited fluorescence spectra with maxima at 350−352 nm. After refolding, the maxima were shifted to 345 and 340 nm, respectively (Figure 2B). Such shifts are consistent with the presence of compact structure in both fragments. When heated in the fluorometer while monitoring the ratio of fluorescence intensity at 370 nm to that at 330 nm as a measure of the spectral shift that accompanies unfolding, both fragments exhibited a sigmoidal transition reflecting unfolding of their compact structure (Figure 3, solid lines). The unfolding process of both fragments was highly reversible since upon cooling the fluorescence ratios returned to a value near the original (Figure 3, dotted lines). These results demonstrate that both recombinant variants were folded into a compact structure.

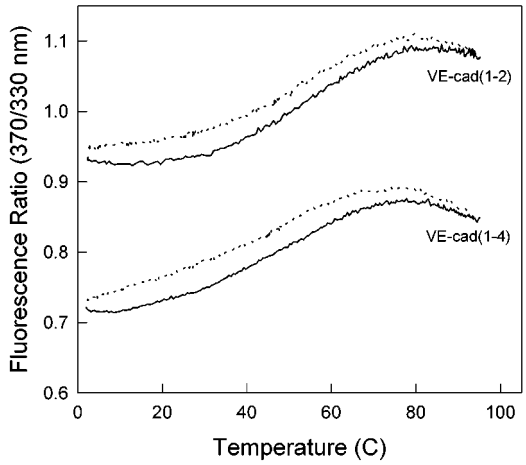

FIGURE 3: Fluorescence-detected thermal unfolding of the recombinant VE-cad(1−2) and VE-cad(1−4) variants. Solid lines represent the change of fluorescence ratio of the fragments upon heating while dotted lines indicate the reversibility upon cooling. The experiments were performed in 20 mM HEPES buffer, pH 7.4, containing 200 mM NaCl and 1 mM $CaCl_2$.

Interaction of the β15−42-Containing Fragments with VE-Cadherin Variants. To test the interaction between the variants of the BβN-domain and the variants of VE-cadherin, the later were immobilized on a BIAcore sensor chip, and the binding of the former was monitored in real time by surface plasmon resonance (SPR). Neither uncleaved nor thrombin-cleaved monomeric and dimeric variants of the BβN-domain, all added at 400 nM, exhibited binding to the immobilized VE-cad(1−2) (not shown). Similarly, none of the monomeric variants of the BβN-domain added at 400 nM, activated or nonactivated, bound to the immobilized VE-cad(1−4) (Figure 4A). However, the thrombin-cleaved dimer, $(\beta 15-66)_2$, added at 200 nM exhibited a prominent binding to the immobilized VE-cad(1−4), while the uncleaved one, $(B\beta 1-66)_2$, failed to bind (Figure 4A). These findings were confirmed in ELISA experiments, in which VE-cad(1−4) bound only to the immobilized activated dimer (Figure 4B). This binding was completely blocked by anti-VE-cadherin monoclonal antibody, Mab-1, (Figure 4B, inset) indicating that it was specific. In agreement, anti-fibrin β chain monoclonal antibody, Mab-2, also inhibited this binding by 64% at the concentration used in the experiment. All these results demonstrate that the VE-cadherin-binding domain in fibrin is composed of two NH_2-terminal portions of the Bβ chains and that the removal of fibrinopeptide B is required to expose its binding site. They also indicate that among two recombinant VE-cadherin variants only VE-cad(1−4) possessed binding activity suggesting that the presence of the third and/or fourth extracellular domains is required for binding of fibrin.

Binding of the VE-cad(1−4) variant to the dimeric $(\beta 15-66)_2$ fragment detected by both ELISA and SPR was dose-dependent. The global fitting analysis (see Experimental Procedures) of the SPR-detected binding curves obtained at various concentrations gave the K_d value of 80 nM (Figure 4A, inset). The value of K_d obtained by fitting the ELISA data was 120 nM (Figure 4B), close to that obtained by SPR. To compare affinity of VE-cad(1−4) to the $(\beta 15-66)_2$ fragment with that to fibrin, fibrinogen was immobilized on a BIAcore sensor chip, converted into fibrin by treatment with thrombin, and increasing concentrations of VE-cad(1−

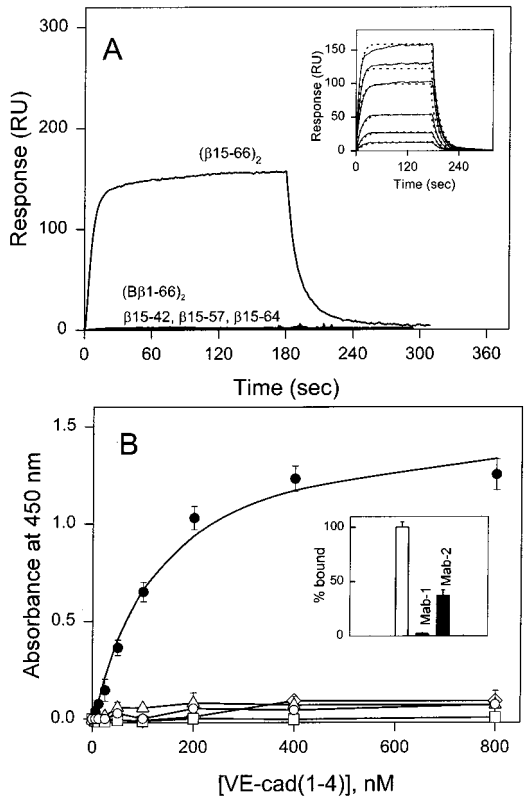

FIGURE 4: Analysis of interaction between the recombinant VE-cad(1−4) variant and the β15−42 containing fibrin(ogen) fragments by surface plasmon resonance (A) and ELISA (B). Panel A, the β15−42, β15−57, and β15−64 fragments at 400 nM, and (Bβ1−66)$_2$ and (β15−66)$_2$ dimers at 200 nM were added to VE-cad(1−4) immobilized on a BIAcore sensor chip and their association/dissociation was monitored in real time while registering the resonance signal (response) using BIAcore biosensor. The curves for the β15−42, β15−57, β15−64, and (Bβ1−66)$_2$ fragments essentially coincide. The inset shows SPR-detected binding of the (β15−66)$_2$ dimer at 6.25, 12.5, 25, 50, 100, and 200 nM to immobilized VE-cad(1−4); the dotted curves represent the best fit of the binding data using global fitting analysis (see Experimental Procedures). The K_d determined from 3 independent experiments was found to be 80 ± 26 nM. Panel B, increasing concentrations of VE-cad(1−4) were incubated with microtiter wells coated with the β15−42 (squares), β15−57 (diamonds), β15−64 (triangles) fragments, and (Bβ1−66)$_2$ dimer (open circles) and thrombin-activated (β15−66)$_2$ dimer (filled circles). Bound VE-cad(1−4) was detected as described in Experimental Procedures. The curve for the (β15−66)$_2$ dimer represents the best fit of the data to eq 1. The K_d determined from three independent experiments was found to be 120 ± 9 nM. The inset in panel B shows the results of the inhibition experiment in which the immobilized (β15−66)$_2$ dimer was incubated at 4 °C overnight with VE-cad(1−4) at 100 nM in the presence (filled bars) or absence (open bar) of the monoclonal antibodies, anti-VE-cadherin Mab-1 or anti-fibrin Mab-2, both at 10 μg/mL. Results are expressed as a percentage of bound VE-cad(1−4). Error bars represent ± SD obtained from three independent experiments.

4) were added. Although some interaction was detected, the data were not reliable due to a high nonspecific binding of VE-cad(1−4) to the surface of the chip (not shown). However, when fibrinogen was immobilized on an IAsys cuvette sensor surface and then converted into fibrin, the nonspecific binding was much lower and the K_d determined using binding data collected at IAsys biosensor was found to be 69 nM (Figure 5A). This value was very close to those determined for the dimer in both BIAcore and IAsys experiments (Figures 4A and 5B, respectively). It should be

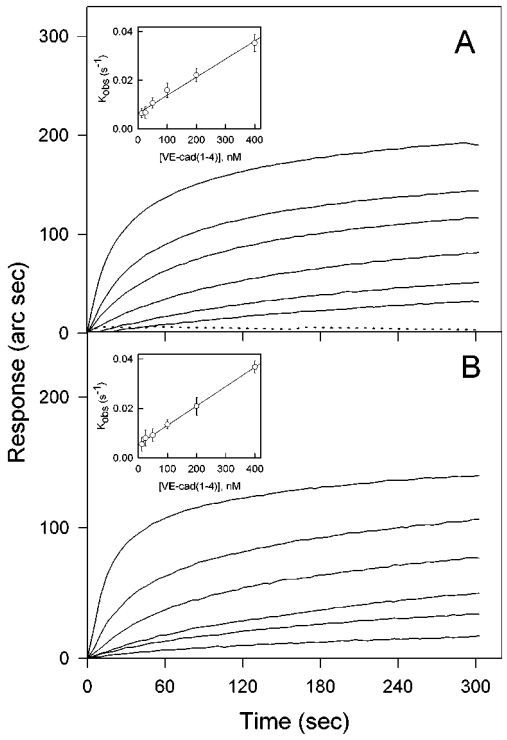

FIGURE 5: Analysis of binding of VE-cad(1−4) to immobilized fibrin(ogen) (A) or the (β15−66)$_2$ dimer (B). Panel A, fibrinogen was immobilized on an IAsys cuvette sensor surface and VE-cad-(1−4) was added at 400 nM to test interaction (dotted line). Fibrinogen was then converted into fibrin by incubation with thrombin and VE-cad(1−4) at concentrations 12.5, 25, 50, 100, 200, and 400 nM was added while registering the resonance signal (solid lines) to monitor association in real time. Panel B, the (β15−66)$_2$ dimer was immobilized on an IAsys cuvette sensor surface and VE-cad(1−4) was added at the same concentrations as above while registering the resonance signal. The inset in each panel shows a plot of the values of k_{obs} determined for each association curve versus ligand concentration to derive k_{ass}, k_{diss} and thus determine the dissociation equilibrium constants, K_d (see Experimental Procedures). The K_d values for the fibrin/VE-cad(1−4) and (β15−66)$_2$/VE-cad(1−4) interactions were found to be 69 ± 23 and 78 ± 10 nM, respectively. Error bars in each inset represent ± SD obtained from two independent experiments. All experiments were performed using IAsys biosensor.

noted that before conversion into fibrin, immobilized fibrinogen exhibited no binding with VE-cad(1−4) added at high concentration (Figure 5A, dotted curve), in agreement with previous studies (*6*, *9*) and with the results for the recombinant β chain fragments presented above. Thus, the affinity of interaction of VE-cad(1−4) with the dimeric (β15−66)$_2$ fragment was comparable to that obtained with fibrin, suggesting that interaction between the activated recombinant (β15−66)$_2$ dimer and the recombinant VE-cad-(1−4) variant mimics well that between fibrin and VE-cadherin.

Interaction of the βN-Domain Mutants with the VE-Cadherin(1−4) Variant. Since removal of the fibrinopeptide B exposes the Gly15−His−Arg−Pro−Leu−Asp20- sequence in the βN-domain of fibrin (*7*), we made several mutations in this region of the (Bβ1−66)$_2$ dimer to further localize the VE-cadherin binding site and to identify critical amino acid residues involved in its formation. Four single mutants with amino acid substitutions H16 → A, R17 → Q, P18 → A, and D20 → N, were produced in *E. coli*. In addition, a double mutant with H16 → P and P18 → V

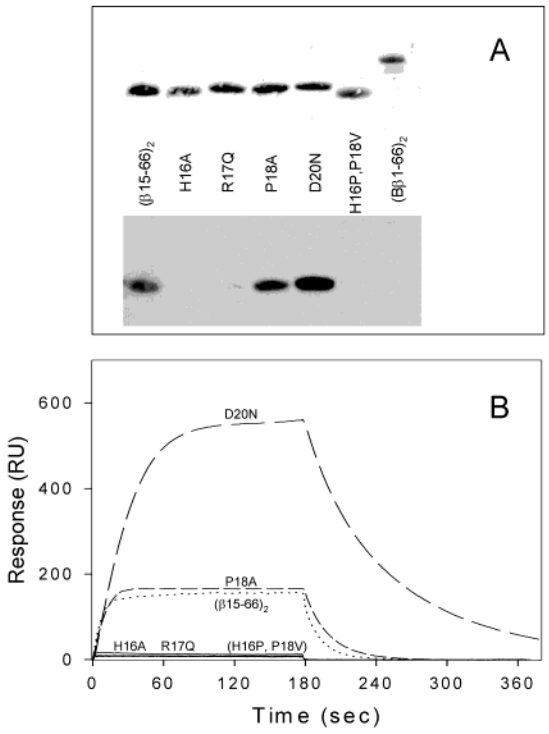

FIGURE 6: Analysis of binding of VE-cad(1−4) to the wild type and mutant $(\beta 15-66)_2$ fragments by ligand blotting (A) and surface plasmon resonance (B). Panel A, the wild type $(\beta 15-66)_2$ and $(B\beta 1-66)_2$ dimers, the mutant H16A, R17Q, P18A, and D20N and double mutant H16P, P18V fragments were transferred to PVDF membrane after SDS-electrophoresis, stained with Ponseau S (top) and then probed with VE-cad(1−4) after de-staining (bottom); bound VE-cad(1−4) was detected as described in Experimental Procedures. Panel B, the wild type and the indicated mutants were added at 200 nM to VE-cad(1−4) immobilized on a BIAcore sensor chip and their association/dissociation was monitored in real time while registering the resonance signal (response) using BIAcore biosensor. The resonance signals for the H16A and R17Q mutants and for the double mutant (H16P, P18V) represented by solid curves essentially coincide.

substitutions was made to mimic the Gly17−Pro−Arg−Val20- sequence which occurs in the homologous position of the Aα chain and which is exposed upon removal of the fibrinopeptide A. All mutants were expressed and purified as described in Experimental Procedures. The mutants were treated with thrombin to remove fibrinopeptide B after which their interactions with VE-cad(1−4) were tested by ligand blotting and SPR.

In a ligand blotting assay, when the wild type $(\beta 15-66)_2$ dimer and its mutants were immobilized on a PVDF membrane after being electrophoresed in SDS-containing polyacrylamide gel, only the wild-type dimer and two single mutants, P18A and D20N, bound VE-cad(1−4), while no binding was observed with the H16A and R17Q single mutants and with the double mutant, H16P, P18V (Figure 6A). This finding was confirmed by SPR measurements in which two mutants, P18A and D20N, bound to the immobilized VE-cad(1−4) while binding of the other mutants at the same concentration (200 nM) was negligible (Figure 6B). The K_d values for these two mutants, determined from the BIAcore analysis of the binding curves obtained in a concentration range of 6.25−200 nM (not shown), were similar to that obtained for the wild type $(\beta 15-66)_2$ dimer, namely, 82 ± 26 nM for P18A and 68 ± 17 nM for D20N. These results indicate that His16 and Arg17 of the fibrin β chain are critical for binding of VE-cadherin while Pro18 and Asp20, which are highly conserved among several vertebrate species, seem to be inert, at least in the studied concentration range.

DISCUSSION

Previous studies revealed that interaction of fibrin with endothelial cell receptor VE-cadherin induces capillary tube formation (*6*, *13*). The present study was performed to further characterize this interaction and to map the VE-cadherin binding site in fibrin. Taking into account that interaction of fibrin(ogen) with endothelial cells occurs through a number of EC receptors and that various regions of fibrin(ogen) are involved in this interaction (*9*, *14*, *16*, *31*), it was necessary to select an appropriate model system that would allow selective testing of the interaction between fibrin and VE-cadherin. This was achieved by producing recombinant domains of both proteins that are involved in this interaction.

The previous suggestions that the β15−42 region of fibrin is involved in binding to VE-cadherin was based mainly on comparative studies of fibrin(ogen) and its N-DSK fragments either containing or lacking this region. Since the isolated β15−42 peptide exhibited rather weak functional activity (*6*, *32*), we first hypothesized that it may not represent the complete functional domain. However, longer versions of this region, the Bβ1−57 and Bβ1−64 fragments, which we selected for expression based on the sequence homology and X-ray data (see Results) also failed to exhibit binding activity after activation with thrombin. At the same time, we discovered that a dimeric disulfide-linked version of this region, the $(\beta 15-66)_2$ dimer, exhibited prominent binding that was comparable to that of fibrin. This result indicates that the VE-cadherin binding site in fibrin, which is a chemical dimer, is also dimeric. It also explains why the β15−42 peptide inhibited capillary tube formation only at very high concentrations (*6*) and why its cross-linking to ovalbumin or immobilization on Sepharose was required for the expression of its binding activity (*8*, *9*). Whether such dimeric structure is required for the expression of other activities by this region remains to be established.

It was suggested that the first and/or second extracellular domains of VE-cadherin participate in heterophilic interaction with fibrin since a monoclonal antibody against residues 26−194 of VE-cadherin (first two domains) inhibited binding of the activated fibrin N-DSK fragment to human umbilical vein endothelial cells (*9*). However, our direct experiments revealed that the recombinant VE-cad(1−2) fragment encompassing first two domains of VE-cadherin exhibited no binding activity toward the $(\beta 15-66)_2$ dimer. At the same time, the recombinant VE-cad(1−4) fragment bound the dimer indicating that the third and/or fourth domains are required for the binding to occur. This suggests that the fibrin-binding site of VE-cadherin may be complex including three or four NH_2-terminal extracellular domains. Alternatively, this may reflect a link between homophilic and heterophilic interactions of VE-cadherin. Namely, since the extracellular domains of VE-cadherin are involved in homophilic interaction (*33*) and the VE-cadherin binding site in fibrin is dimeric (this study), one can speculate that dimerization of VE-cadherin is required for its heterophilic interaction with fibrin and that its first and/or second domains

may be important for dimerization, while the third and/or fourth ones are involved in fibrin binding. In agreement, it was suggested that the first domain of the other members of the cadherin family is responsible for homophilic recognition (*34*, *35*). It was also reported recently that monoclonal antibodies directed to the first, third, and forth domains of VE-cadherin affect its homophilic interaction (*36*). The latter suggests that the relationship between the homophilic and heterophilic interactions of VE-cadherin may be even more complex than speculated above. The model system described in this study may be a useful tool to test these speculations and to localize fibrin-binding site(s) in VE-cadherin and further clarify the mechanism of its interaction with fibrin.

Having an appropriate model system that allowed easy testing of the interaction between fibrin and VE-cadherin and manipulation of the sequence, we mutated several residues in the NH_2-terminal region of the $(\beta 15-66)_2$ dimer and tested binding of the mutants to VE-cad(1−4). The results revealed that mutation of His16 and Arg17 totally abrogated binding while mutation of Pro18 and Asp20 had no effect. Thus the newly exposed Gly−His−Arg−Pro-(GHRP-) sequence in fibrin represents either part of or the entire VE-cadherin binding site and His16 and Arg17 are critical residues for the binding. It is interesting that these residues are involved in formation of the GHRP-containing secondary polymerization site whose interaction with the complementary site in the D region contributes to the lateral aggregation of protofibrils upon fibrin assembly (*37*). This means that in fibrin this sequence should be occupied. However, the measurements with monoclonal antibody specific to this sequence revealed that in a fibrin gel about 14% of the sites are exposed (*38*). This suggests that the GHRP-containing polymerization sites in at least some fibrin molecules are not involved in interaction with the complementary polymerization sites, most probably in those that are located on the surface of fibers. Thus, when unoccupied, they interact with VE-cadherin inducing formation of capillary tubes.

Besides capillary tube formation, interaction of fibrin with endothelial cells induces a number of cellular responses including cell spreading and proliferation (*39*, *40*), release of von Willebrand factor (*8*), and upregulation of ICAM-1 (*41*). It seems the same region of fibrin, namely, its newly exposed β chain 15−42 sequence, is required for these activities to occur. However, it is still unclear whether all these activities are connected with the interaction of the fibrin βN-domain with VE-cadherin or some other receptors are involved, and whether these putative receptors share the same binding site within the βN-domain. The $(\beta 15-66)_2$ dimer prepared in this study provides a useful tool to address these questions.

ACKNOWLEDGMENT

We thank Dr. S. Lord for providing full-length cDNA of the Bβ chain of human fibrinogen, and Dr. J. Martinez for providing full-length cDNA of human VE-cadherin. We also thank Dr. K. Ingham for helpful discussions and criticism.

REFERENCES

1. Folkman, J. (2001) *Cancer Invest. 19*, 732−738.
2. Ware, J. A., and Simons, M. (1997) *Nat. Med. 3*, 158−164.
3. Tonnesen, M. G., Feng, X., and Clark, R. A. (2000) *J. Invest. Dermatol. Symp. Proc. 5*, 40−46.
4. Conway, E. M., Collen, D., and Carmeliet, P. (2001) *Cardiovasc. Res. 49*, 507−521.
5. Dvorak, H. F., Harvey, V. S., Estrella, P., Brown, L. F., McDonagh, J., and Dvorak, A. M. (1987) *Lab. Invest. 57*, 673−686.
6. Chalupowicz, D. G., Chowdhury, Z. A., Bach, T. L., Barsigian, C., and Martinez, J. (1995) *J. Cell Biol. 130*, 207−215.
7. Henshen, A., and McDonagh, J. (1986) in *Blood Coagulation* (Zwaal, R. F. A., and Hemker, H. C., Eds.) pp 171−241, Elsevier Science Publishers, Amsterdam.
8. Erban, J. K., and Wagner, D. D. (1992)*J. Biol. Chem. 267*, 2451−2458.
9. Bach, T.L., Barsigian, C., Yaen, C.H., and Martinez, J. (1998) *J. Biol. Chem. 273*, 30719−30728.
10. Suzuki, S., Sano, K., and Tanihara, H. (1991) *Cell Regul. 2*, 261−270.
11. Lampugnani, M. G., Resnati, M., Raiteri, M., Pigott, R., Pisacane, A., Houen, G., Ruco, L. P., and Dejana, E. J. (1992) *Cell Biol. 118*, 1511−1522.
12. Gulino, D., Delachanal, E., Concord, E., Genoux, Y., Morand, B., Valiron, M. O., Sulpice, E., and Scaife, R. (1998) *J. Biol. Chem. 273*, 29786−29793.
13. Bach, T. L., Barsigian, C., Chalupowicz, D. G., Busler, D., Yaen, C. H., Grant, D. S., and Martinez, J. (1998) *Exp. Cell. Res. 238*, 324−334.
14. Cheresh. D. A., Berliner, S. A., Vicente, V., and Ruggeri, Z. M. (1989) *Cell 58*, 945−53.
15. Languino, L. R., Plescia, J., Duperray, A., Brian, A. A., Plow, E. F., Geltosky, J. E., and Altieri, D. C. (1993) *Cell 73*, 1423−1434.
16. Yokoyama, K., Zhang, X. P., Medved, L., and Takada, Y. (1999) *Biochemistry 38*, 5872−5877.
17. Smith, R. A., Rooney, M. M., Lord, S. T., Mosesson, M. W., and Gartner, T. K. (2000) *Thromb. Haemostasis 84*, 819−825.
18. Odrljin, T. M., Francis, C. W., Sporn, L. A., Bunce, L. A., Marder, V. J., and Simpson-Haidaris, P. J. (1996) *Arterioscler. Thromb. Vasc. Biol. 16*, 1544−1551.
19. Skogen, W. F., and Wilner, G. D. (1986*) Thromb. Res. 41*, 161−166.
20. Bolyard, M. G., and Lord, S. T. (1989) *Blood 73*, 1202−1206.
21. Yaen, C. H., Ferber, A., Bach, T. L., and Martinez, J. (1999) *Thromb. Haemostasis* Suppl., 207.
22. Edelhoch, H. (1967) *Biochemistry* 6, 1948−1954.
23. Gill, S. C., and von Hippel, P. H**.** (1989) *Anal. Biochem. 182*, 319−326.
24. Karlsson, R., and Falt, A. (1997) *J. Immunol. Methods 200*, 121−133.
25. Hall, D. (2001) *Anal. Biochem. 288*, 109−125.
26. Morton, T. A., and Myszka, D. G. (1998) *Methods Enzymol. 295*, 268−294.
27. Gorgani, N. N., Parish, C. R., and Altin, J. G. (1999) *J. Biol. Chem. 274*, 29633−29640.
28. Madrazo, J., Brown, J. H., Litvinovich, S., Dominguez, R., Yakovlev, S., Medved, L., and Cohen, C. (2001) *Proc. Natl. Acad. Sci. U.S.A. 98*, 11967−11972.
29. Yang, Z., Kollman, J. M., Pandi, L., and Doolittle, R. F. (2001) *Biochemistry 40*, 12515−12523.
30. Pandya, B. V., Gabriel, J. L., O'Brien, J., and Budzynski, A. Z. (1991) *Biochemistry 30*, 162−168.
31. Altieri, D. C., Duperray, A., Plescia, J., Thornton, G. B., and Languino, L. R. (1995) *J. Biol. Chem. 270*, 696−699.
32. Martinez, J., Ferber, A., Bach, T. L., and Yaen, C. H. (2001) *Ann. N. Y. Acad. Sci. 936*, 386-405.
33. Breviario, F., Caveda, L., Corada, M., Martin-Padura, I., Navarro, P., Golay, J., Introna, M., Gulino, D., Lampugnani, M. G., and Dejana, E. (1995) *Arterioscler. Thromb. Vasc. Biol. 15*, 229−239.

34. Nose, A., Tsuji, K., and Takeichi, M. (1990) *Cell 61*, 147−155.
35. Shapiro, L., Fannon, A. M., Kwong, P. D., Thompson, A., Lehmann, M. S., Grubel, G., Legrand, J. F., Als-Nielsen, J., Colman, D. R., and Hendrickson, W. A. (1995) *Nature 374*, 327−337.
36. Corada. M., Liao, F., Lindgren, M., Lampugnani, M. G., Breviario, F., Frank, R., Muller, W. A., Hicklin, D. J., Bohlen, P., and Dejana, E. (2001) *Blood 97*, 1679−1684.
37. Yang, Z., Mochalkin, I., and Doolittle, R. F. (2000) *Proc. Natl. Acad. Sci. U.S.A. 97*, 14156−14161.
38. Procyk, R., Kudryk, B., Callende, r S., and Blomback, B. (1991) *Blood 77*, 1469−1475.
39. Bunce, L. A., Sporn, L. A., and Francis, C. W. (1992) *J. Clin. Invest. 89*, 842−850.
40. Sporn, L. A., Bunce, L. A., and Francis, C. W. (1995) *Blood 86*, 1802−1810.
41. Harley, S. L., Sturge, J., and Powell, J. T. (2000) *Arterioscler. Thromb. Vasc. Biol. 20*, 652−658.

BI0160314